IJCRT.ORG ISSN : 2320-2882

INTERNATIONAL JOURNAL OF CREATIVE RESEARCH THOUGHTS (IJCRT)

An International Open Access, Peer-reviewed, Refereed Journal

DESIGN AND IMPLEMENTATION OF A SOLAR POWERED MULTIPURPOSE AGRICULTURAL ROBOT USING ATMEGA328 AND 433 MHz RF CONTROL

[1]Dahibhate Pooja Pratap, [2]Prof. J.S.Hatte

[1]M.Tech. Student, [2] Professor

[12]Electronic and communication Engineering

[12]M.S.Bidve Engineering College, Latur, India

Abstract: Indian agriculture continues to depend heavily on manual labour and small fuel-powered implements for repetitive field operations such as soil digging, weed removal and crop cutting. Rising fuel prices, seasonal labour scarcity and the emissions associated with small engine-driven machinery have created a need for low-cost, energy-autonomous field equipment suited to small and medium landholdings. This paper presents the design, implementation and experimental evaluation of a solar-powered multipurpose agricultural robot that performs movement, digging and cutting operations under wireless remote control. The implemented prototype harvests energy through a 12 V, 5 W photovoltaic panel that charges a 12 V, 1.2 Ah rechargeable battery; a three-terminal series regulator derives the 5 V logic rail while the battery rail supplies the actuators directly. An ATmega328P microcontroller, operating with a 16 MHz crystal oscillator and an external reset network, interprets commands received through a 433 MHz RF receiver and drives two L293D H-bridge motor drivers. The first driver controls four base motors arranged as left and right traction groups; the second operates the cutter and shaft actuators. The operator unit comprises four push buttons, a parallel-to-serial encoder and a 433 MHz transmitter with antenna. Testing of the assembled prototype reported a battery charging time of 4–5 hours of sunlight, 6–8 hours of continuous operation, a stable radio link over 50–100 m in open field with less than 1% signal loss, a base traversal speed of approximately 0.2 m/s, cutter and shaft speeds of 200–300 rpm, and a 70% reduction in manual labour on the test plots, with zero fuel consumption throughout. The results demonstrate the feasibility of solar-assisted, RF-controlled multipurpose field robots for small-scale agriculture.

Index Terms – Solar energy, Agricultural robot, ATmega328, 433 MHz RF communication, L293D motor driver, Renewable energy, Agricultural automation, Remote-controlled robot.

I. INTRODUCTION

Agriculture remains the principal livelihood for a large share of the rural population in India and in most developing economies, yet the operations that dominate the crop cycle have changed comparatively little. Land preparation, weeding, inter-cultivation and harvesting are still executed either by hand or with small fuel-driven implements. Both approaches have become progressively less viable. Seasonal migration and the movement of rural labour towards non-farm employment have made skilled field labour scarce and expensive at exactly the times of year when it is most needed, while the price of diesel and the maintenance burden of small internal-combustion machinery erode the already thin margins available to smallholders.

The environmental cost of conventional mechanisation compounds the economic one. Small diesel tillers and engine-driven cutters operate at low thermal efficiency and emit particulate matter and oxides of nitrogen directly into the working environment of the operator, while their weight contributes to soil compaction on small, frequently worked plots. For holdings of one or two hectares such machines are also frequently oversized for the task actually performed, so that fuel is consumed transporting mass rather than doing useful work.

Agricultural robotics offers a route past this impasse. A light, purpose-built machine that carries only the actuators required for a specific operation can perform that operation at a fraction of the energy cost of a general-purpose tractor-mounted implement, and can be operated by a single person without specialised training. When such a machine is powered from a photovoltaic source, the recurring fuel cost falls to zero and the system becomes usable in locations where the electricity grid is unreliable or absent — a condition that still characterises a considerable fraction of Indian farmland. Solar generation is also well matched to the agricultural duty cycle, since field work and peak insolation occur within the same daylight window.

Full autonomy, however, imposes requirements that a low-cost prototype cannot economically satisfy. Autonomous row-following, obstacle avoidance and task planning depend on sensing, localisation and computational resources whose cost typically exceeds that of the mechanical platform itself, and whose reliability in dust, vibration and variable illumination is difficult to guarantee. A remote-controlled architecture retains the operator in the decision loop while still removing the operator from the physical hazards of the working implement, and does so at a component cost compatible with small-farm economics. This intermediate position — mechanised and energy-autonomous, but operator-directed — is the design point addressed in this work.

This paper presents the design, hardware implementation and experimental evaluation of a solar-powered multipurpose agricultural robot. The implemented prototype integrates five subsystems: a photovoltaic generation and battery storage stage, a regulated power distribution stage, an ATmega328P microcontroller acting as the central controller, a 433 MHz radio-frequency link providing wireless command reception, and a pair of L293D H-bridge drivers that operate four base traction motors together with cutter and shaft actuators for cutting and digging. The complete signal path therefore runs from a hand-held button panel, through an encoder and RF transmitter, to the receiver, microcontroller, motor drivers and finally the agricultural tools.

The contributions of this work are as follows. First, a complete and reproducible hardware realisation of a solar-assisted, RF-controlled multipurpose field robot is described at the level of subsystem, circuit and printed-circuit-board integration. Second, the control architecture that maps a four-button remote command set onto two independent H-bridge driver stages, allowing traction and tool actuation to be commanded separately, is documented. Third, the assembled prototype is evaluated experimentally for power autonomy, wireless link reliability, actuator performance and agricultural task execution, and the reported measurements are analysed to establish where the approach is practically viable and where its present limitations lie.

II. Literature Review

Research on renewable-energy-powered agricultural robotics has expanded rapidly, and several of the reported systems are directly comparable to the platform described here in their power architecture, controller choice or functional scope.

Kamble et al. [1] developed a solar-powered agricultural robot capable of performing multiple farming tasks, using a 12 V photovoltaic panel with Arduino-based control to manage soil tilling and seeding. The work reported meaningful reductions in fuel consumption and labour cost, confirming that a panel of this class can sustain light field actuation. Its stated limitations were a restricted remote-control range and degraded battery endurance under overcast conditions, both of which bear directly on the design decisions taken in the present implementation: the choice of a 433 MHz link rather than a shorter-range modality, and the sizing of the storage battery so that operation continues after generation ceases.

Patil et al. [2] described a solar-powered multipurpose agriculture robot supporting ploughing, weeding and spraying. Their controller and driver arrangement closely resembles the configuration adopted here, based on an ATmega328 device with discrete motor drivers, which makes their reported difficulties particularly relevant. Command transfer in that system relied on a Bluetooth link, which the authors found susceptible to interference and range loss in open-field conditions, and the platform's traction arrangement limited performance on rugged terrain. These observations motivated the use of a dedicated 433 MHz RF channel and a four-motor base in the present work.

Chadalavada [3] presented a solar-powered semi-automated multipurpose agriculture tool combining photovoltaic supply with digging and cutting mechanisms. The contribution of that study is primarily its demonstration of cost-effectiveness for smallholder use, establishing that the mechanical functions targeted here can be sustained from a modest solar budget. The tool was, however, only semi-automated and lacked a remote-operation capability, so the operator remained adjacent to the working implement throughout.

Further implementations reported in the applied engineering literature reinforce these conclusions. Beldar et al. [4] describe a solar-powered, multi-use, remote-controlled farm robot; the work reported in [5] and [6] addresses solar-powered automated multi-tasking agricultural platforms; and the web-controlled multi-function agribot described in [7] extends the command interface to a networked channel. Collectively these studies establish the technical viability of photovoltaic supply for small agricultural machines and the adequacy of low-cost 8-bit microcontrollers for coordinating several actuators.

A. Identified Research Gap

Read together, the reviewed works leave four issues insufficiently resolved. Wireless control reliability remains the most consistent weakness: systems using short-range or consumer-protocol links report interference and range collapse in open fields, where line-of-sight distances of several tens of metres are routinely required. Multipurpose functionality is frequently claimed but is often implemented as a single tool head, so that traction and tool actuation contend for the same driver stage. Energy management is generally addressed at the level of panel selection rather than as an explicit balance between charging duration and usable operating duration. Finally, few reports document practical field operation of a compact, low-cost build at a level of detail sufficient for reproduction.

The system described in this paper addresses these gaps by pairing a dedicated 433 MHz link with an architecture in which traction and tool actuation are assigned to separate H-bridge drivers, and by reporting charging and operating durations as measured quantities rather than design targets. It should be stated explicitly that the implemented prototype is remotely operated and not autonomous; no navigation sensing, localisation or decision-making capability is present in the build reported here.

III. PROPOSED SYSTEM

A. System Architecture

The system is partitioned into two physically separate units: a hand-held transmitter carried by the operator and a receiver unit mounted on the robot chassis. The two units share no wired connection; all command transfer occurs over the 433 MHz radio channel.

On the robot side, the energy path and the signal path converge at the microcontroller. Energy flows from the photovoltaic panel to the storage battery, from the battery to a three-terminal series regulator, and from the regulator to the logic-level subsystems. The unregulated battery rail is routed separately to the motor supply pins of the driver stages, so that the inrush and commutation transients of the actuators are not imposed on the controller supply. The signal path runs from the RF receiver into the microcontroller port pins, and from the microcontroller output pins into the two H-bridge drivers, which in turn energise the base motors and the cutter and shaft motors. The receiver-side architecture is therefore:

Solar Panel → Battery → Voltage Regulator → ATmega328P ← RF Receiver; ATmega328P → Motor Drivers → Base Motors / Cutter Motor / Shaft Motor

The transmitter unit is deliberately minimal. Four momentary push buttons are presented to the operator; their parallel states are converted into a serial command word by an encoder stage, modulated by the 433 MHz transmitter module and radiated through a whip antenna. The transmitter is powered by its own battery and is independent of the robot's energy system:

Push Buttons → Parallel-to-Serial Encoder → 433 MHz RF Transmitter → Antenna

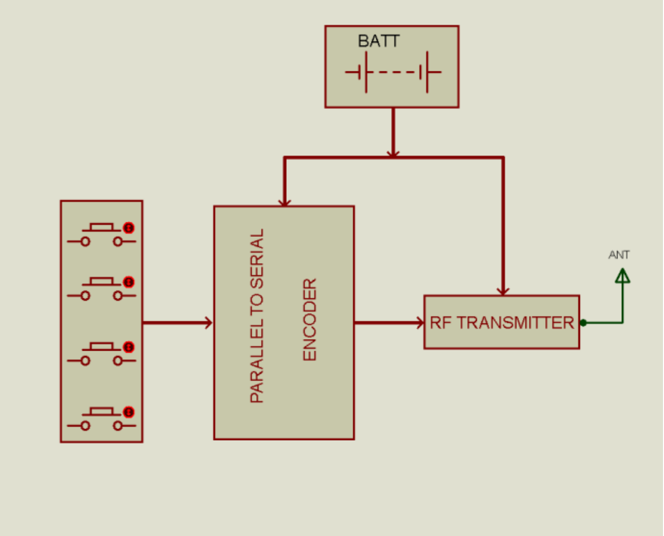

Fig. 1. Transmitter-side (user end) block diagram of the implemented remote control unit.

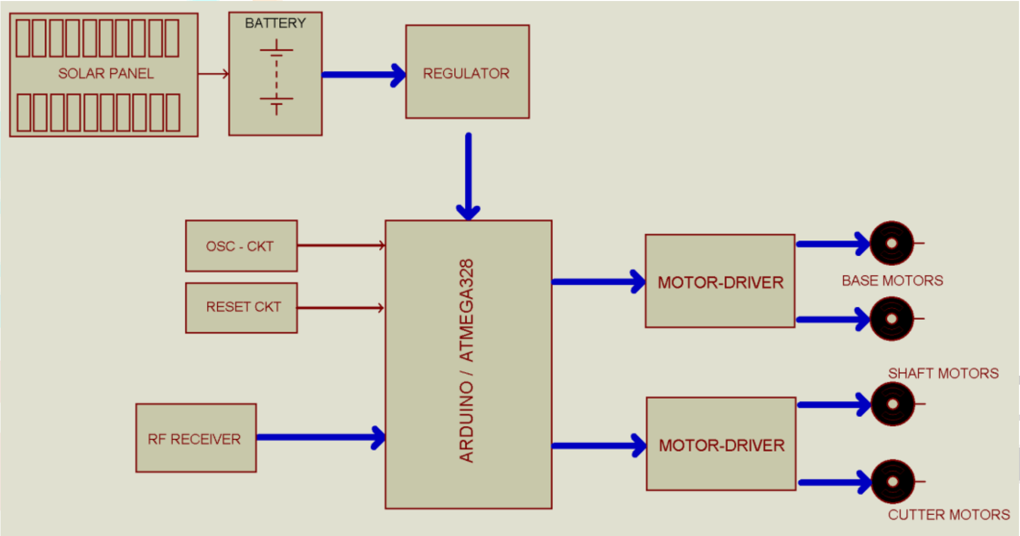

Fig. 2. Receiver-side (robot end) block diagram showing the solar generation, storage, regulation, control and actuation stages.

B. Transmitter–Receiver Interaction

Communication is unidirectional. While a button is held, the encoder continuously generates the corresponding command word and the transmitter radiates it; the receiver demodulates the incoming stream and presents the recovered bits to the microcontroller port pins. The controller interprets the received pattern and asserts the matching combination of driver inputs. Because the link carries no return channel, the robot provides no status telemetry to the operator, and control is exercised by direct visual observation of the machine in the field. When transmission ceases, the received pattern reverts to its idle state and the driver inputs are de-asserted, so that the actuators stop. This behaviour provides an inherent fail-safe: loss of the radio link results in the machine coming to rest rather than continuing its last commanded action.

IV. Hardware Implementation

A. Solar Power System

Generation is provided by a 12 V, 5 W photovoltaic panel mounted on the upper surface of the chassis. The panel output is connected through a switch to the terminals of a 12 V, 1.2 Ah rechargeable battery, which serves as the sole energy buffer for the platform. This direct-coupling arrangement is characteristic of small photovoltaic systems in which the panel's short-circuit current is low relative to the battery capacity, so that the battery itself constrains the charging current.

The battery rail feeds two distinct distribution paths. The first passes through a 78XX-series three-terminal positive regulator, which supplies the 5 V logic rail used by the microcontroller, the RF receiver and the logic supply pins of the driver stages. This device provides internal current limiting, thermal shutdown and safe-operating-area protection, which is significant in a machine subject to stall conditions at the actuators. Bulk and decoupling capacitors are distributed across both sides of the regulator to stabilise the rails against the switching transients generated by the motors. The second path carries the unregulated 12 V battery voltage directly to the motor supply inputs of the H-bridge drivers.

The machine's energy autonomy therefore derives entirely from ambient solar radiation: no grid connection, fuel supply or external charging infrastructure is required during operation, which is the principal enabling condition for deployment where electricity supply is limited or intermittent. No conversion-efficiency figures for the panel or the regulation stage are reported in the available project documentation, and none are estimated here.

B. ATmega328P Microcontroller

The ATmega328P operates as the central controller of the platform. It is configured with an external 16 MHz crystal oscillator and its associated loading capacitors on the oscillator pins, and with a resistor–capacitor reset network on the reset input to ensure deterministic start-up when supply voltage is applied through the mechanical switch. The supply and analogue supply pins are tied to the regulated 5 V rail with a common ground reference shared across the controller, receiver and driver logic.

Functionally the controller performs four tasks. It samples the port pins connected to the RF receiver outputs to acquire the current command state; it interprets that state as one of the defined operations — forward, reverse, left turn, right turn, cutter actuation or shaft actuation; it drives the corresponding input pins of the two H-bridge drivers to produce the required direction and enable pattern; and it de-asserts all driver inputs when no valid command is present. The device was chosen for the implementation because it provides a sufficient number of general-purpose digital pins for two independent four-input driver stages plus the receiver interface, while remaining programmable through the standard Arduino toolchain and available at low unit cost.

C. 433 MHz RF Communication Subsystem

Wireless command transfer uses a matched 433 MHz transmitter and receiver module pair. On the transmitter side, the encoder converts the parallel button states into a serial word that modulates the carrier; on the receiver side, the demodulated bits are presented on parallel output lines connected to the microcontroller port pins. The 433 MHz band was selected for its favourable propagation over open ground and around low vegetation, its tolerance of partial obstruction relative to higher-frequency consumer links, and the low cost and minimal supporting circuitry of the available modules.

The command set is directional and discrete rather than proportional: each button corresponds to one operation, and the operation persists for as long as the button is held. In testing, the link sustained reliable operation at separations of 50 to 100 m in open field, with less than 1% signal loss observed. Antennas are fitted at both ends of the link; range is dependent on antenna orientation, terrain and the presence of other emitters in the band.

D. L293D Motor Driver Stages

Two L293D quadruple half-H drivers form the interface between the controller's logic-level outputs and the motor loads. Each device accepts logic inputs and enable signals from the microcontroller and switches the 12 V motor rail to the corresponding output terminals, providing the current gain and the bidirectional switching capability that the controller cannot supply directly. Reversing the logic state across an H-bridge pair reverses the polarity applied to the motor and hence its direction of rotation; de-asserting both inputs of a pair leaves the motor unenergised.

The first driver is assigned to the base motors, with the left-hand and right-hand motor groups connected to separate bridge pairs so that differential actuation produces turning. The second driver is assigned to the tool actuators, operating the shaft motor for digging and the cutter motor for cutting. Separating traction from tool actuation in this way means that the current drawn by a stalled or heavily loaded cutter does not directly constrain the traction stage. The L293D incorporates internal thermal shutdown, which was relied upon during testing: minor overheating was observed under sustained load and was managed through the device's built-in protection.

E. DC Motors and Drive Configuration

Four DC geared motors provide traction, arranged as left and right drive groups. Forward and reverse motion is produced by driving both groups in the same sense; turning is produced by driving them in opposition or by de-energising one group. Gear reduction is used in preference to direct drive because field traction requires torque rather than rotational speed, and because a reduced output speed simplifies the control of a machine commanded by discrete button presses. In testing, the base traversal speed was approximately 0.2 m/s.

Two further motors carry the agricultural tools. The cutter motor drives the cutting element and the shaft motor drives the digging element; both were observed to operate in the range of 200 to 300 rpm during testing, which was found adequate for the cutting and digging operations performed on the test plots.

F. Agricultural Tool Mechanisms

Three agricultural functions are implemented on the prototype. Movement is provided by the four-motor base, which allows the machine to be positioned and traversed across the plot under operator command. Digging is provided by the shaft-driven element, which engages the soil surface for loosening and preparation. Cutting is provided by the cutter-driven element, used for trimming and weed removal within crop rows. Each function is commanded independently from the remote unit, and traction and tool operation may be exercised concurrently because they are driven from separate H-bridge stages.

A pump output is present in the circuit design, driven through a transistor stage from a controller output pin and intended for irrigation. This output forms part of the implemented schematic; however, no irrigation testing or pump performance data appears in the available project documentation, and the capability is therefore reported here as provided-for in the circuit design rather than as an experimentally validated function.

V. Circuit and Control Implementation

The implemented circuit integrates the solar power subsystem, the ATmega328P controller, the RF receiver, the two motor-driver stages and the agricultural actuators on a single board, enabling wireless control of the robot from the hand-held transmitter. The complete schematic is shown in Fig. 3.

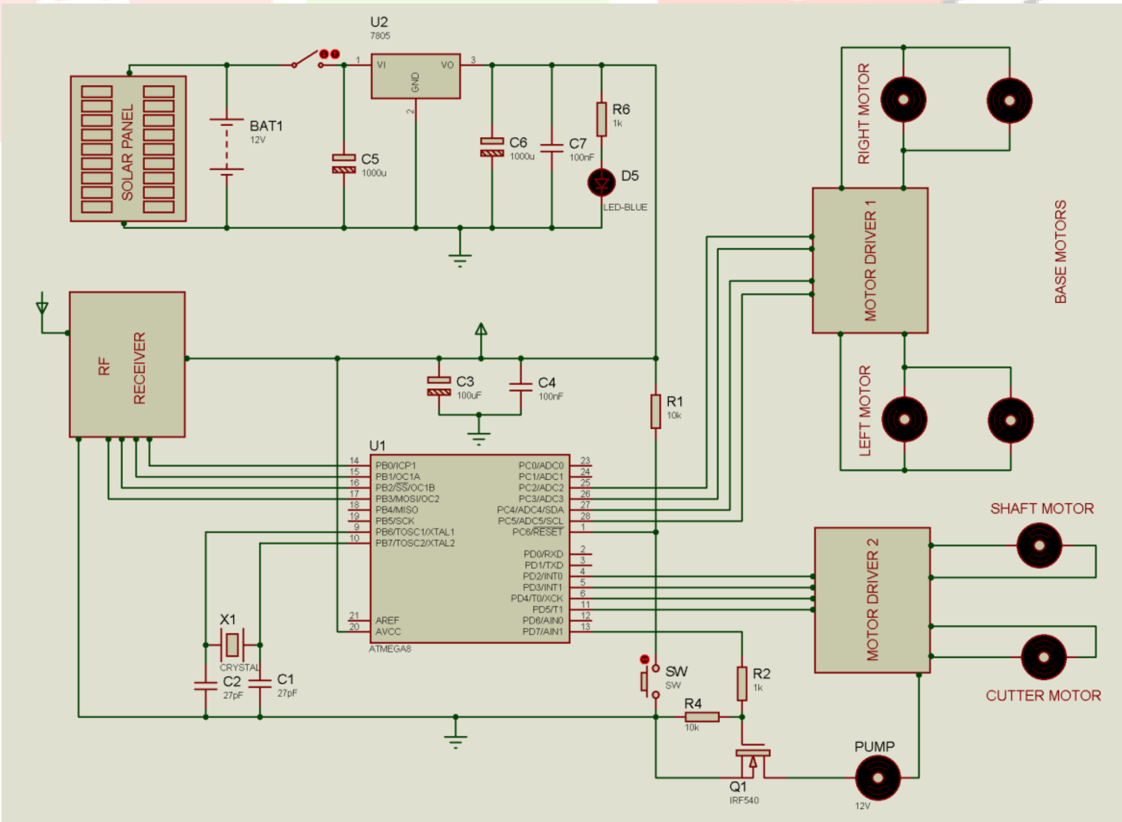

Fig. 3. Circuit diagram of the implemented receiver-side system, showing the solar and battery supply, regulator, ATmega328P controller with oscillator and reset network, RF receiver, and the two motor-driver stages.

In the power-supply section, the panel and the 12 V battery are connected through a manual switch to the input of the three-terminal regulator. Bulk electrolytic and ceramic capacitors are placed at the regulator input and output to suppress ripple and to provide local charge storage during motor switching transients, and an indicator light-emitting diode with its series resistor confirms the presence of the regulated rail. The regulated output supplies the controller, the receiver and the driver logic, while the battery rail supplies the driver output stages.

The controller section comprises the ATmega328P with its crystal oscillator connected across the oscillator pins together with the associated loading capacitors, and the reset input held through a pull-up resistor with provision for manual reset. The RF receiver module is supplied from the regulated rail and its recovered data outputs are connected to a group of controller port pins, so that the received command word is available as a parallel pattern at the input port.

In the actuation section, one group of controller output pins drives the input and enable terminals of the first L293D, whose outputs are connected to the right-hand and left-hand base motors; a second group drives the input terminals of the second L293D, whose outputs are connected to the shaft motor and the cutter motor. A further controller output drives a power MOSFET through a gate resistor to switch the 12 V pump load. Supporting components include current-limiting and pull-up resistors, decoupling capacitors distributed across the supply rails, and the indicator diode.

The end-to-end signal flow is therefore: a remote command is issued at the button panel; the encoder and 433 MHz transmitter radiate the corresponding word; the RF receiver demodulates it; the ATmega328P interprets the recovered pattern; the appropriate motor driver is enabled with the required direction inputs; the selected motor or motor group is energised; and the corresponding agricultural operation is performed.

VI. Software and Control Logic

The firmware executing on the ATmega328P implements a continuous input-sampling loop with no autonomous decision-making. Its behaviour is fully determined by the command pattern presented at the receiver interface, and the control sequence proceeds as follows. The operator presses a directional or tool button on the remote unit. The encoder converts the parallel button state into a serial command word. The 433 MHz transmitter radiates the modulated word. The receiver on the robot demodulates the transmission and presents the recovered bits at the controller port. The controller reads the port, compares the pattern against the defined command set and selects the corresponding output configuration. The relevant driver inputs are asserted, energising the base motors for traversal or the cutter and shaft motors for tool operation. The commanded operation continues while the pattern persists; when the pattern reverts to its idle state, the driver inputs are de-asserted and the motors stop.

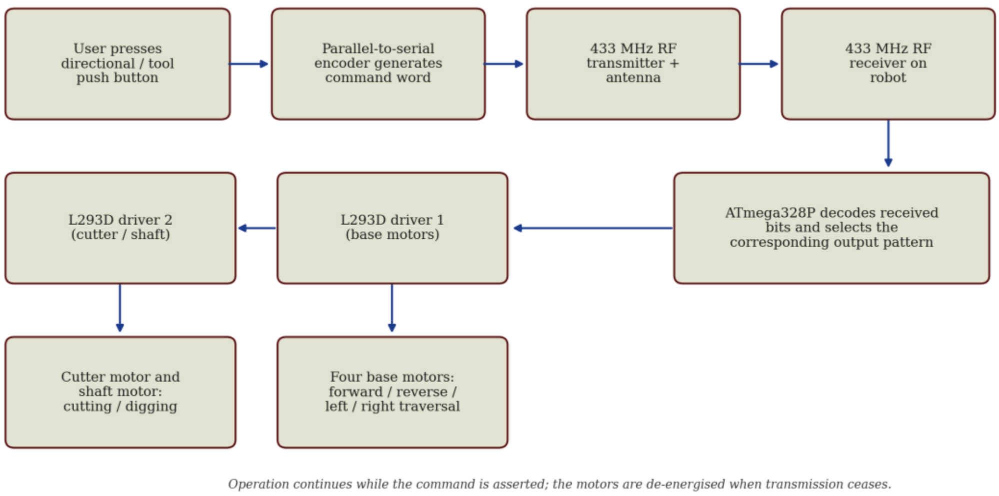

Fig. 4. Control and signal flow of the implemented system, from operator command to agricultural operation.

The Arduino source code for the prototype is not contained in the available project documentation, and no listing is reproduced here. The control behaviour described above can be summarised in the following pseudocode, which is provided as a description of the logic rather than as the firmware actually deployed:

initialise:

```
    configure receiver-interface pins as inputs
    configure driver-interface pins as outputs
    de-assert all driver inputs

loop forever:
    command <- read receiver interface pins

    if command = FORWARD:
        drive left group and right group in forward sense
    else if command = REVERSE:
        drive left group and right group in reverse sense
    else if command = LEFT:
        drive right group forward, left group stopped or reversed
    else if command = RIGHT:
        drive left group forward, right group stopped or reversed
    else if command = CUTTER:
        enable cutter bridge on driver 2
    else if command = SHAFT:
        enable shaft bridge on driver 2
    else:
        de-assert all driver inputs      // no valid command: stop
```

Two properties of this structure are worth noting. First, the machine holds no internal state between iterations: each pass of the loop re-evaluates the received command and reconfigures the outputs accordingly, so an interrupted transmission cannot leave an actuator latched on. Second, the default branch enforces the fail-safe behaviour described in Section III, since absence of a valid command is treated identically to an explicit stop instruction.

VII. PCB Design and Hardware Integration

The controller, RF receiver, regulation stage and motor-control interconnections were consolidated onto a single printed circuit board in order to eliminate the loose wiring that would otherwise be exposed to the vibration and dust of field operation. Component placement follows the functional partitioning of the schematic: the supply and regulation components occupy one region of the board with short, wide tracks between the battery input, the regulator and the bulk capacitors; the controller with its oscillator and reset network occupies the central region, with the oscillator components placed close to the device pins to limit stray capacitance on the clock nodes; and the receiver and the driver interfaces are brought out to connector headers at the board periphery so that the motor harness and the receiver module can be detached during servicing.

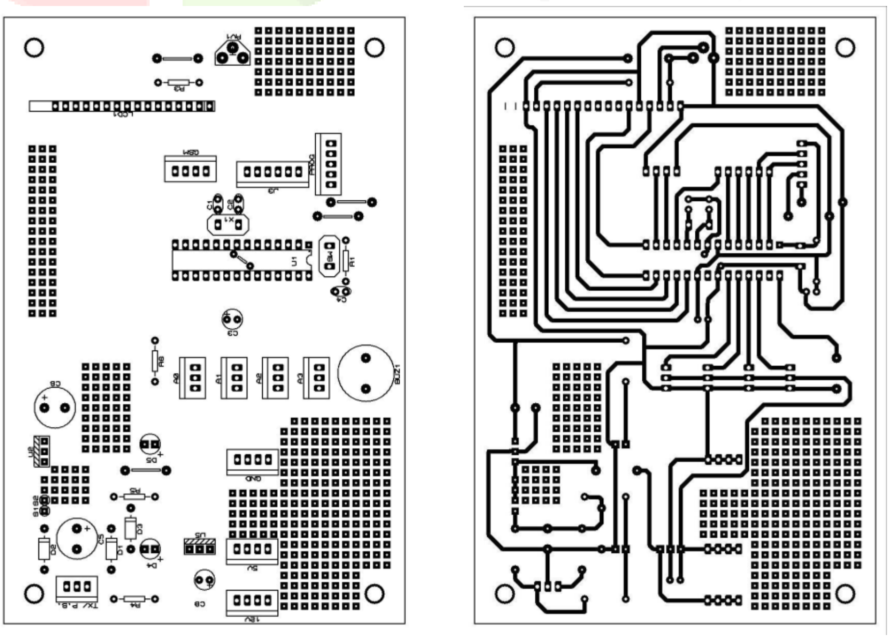

Fig. 5. Printed circuit board artwork used for hardware integration: (a) top-side component layout and (b) bottom-side copper track layout.

The board artwork reproduced in Fig. 5 corresponds to a general-purpose ATmega328P controller board carrying the microcontroller socket, oscillator and reset components, the regulated supply section and the connector headers used in this build. It additionally provides several unpopulated footprints, including display and serial-module headers, which were not used in the present implementation.

Two fabrication routes are described in the project documentation: photo printing and screen printing. Photo printing offers higher dimensional accuracy at greater cost, while the screen process — adopted for this build — applies a resist ink through a stencil mounted on a fine mesh screen, transferring a positive image of the conductor pattern onto the copper foil of the blank board. The stencil is produced from pre-sensitised film exposed against the artwork, developed, washed out and adhered to the screen. After the resist has dried, the board is etched to remove the unprotected copper; ferric chloride is identified as the preferred etchant on grounds of cost, availability and comparative safety, with the etchant maintained at elevated temperature to keep etching times consistent. Component holes are then drilled, with drill speed selected according to the laminate in use, before component insertion and soldering.

Integration proceeds by populating the passive components and sockets first, followed by the regulator and the controller, and finally by attaching the receiver module, the motor harness and the battery and panel leads at the connector headers. No board dimensions, track widths or fabrication tolerances are recorded in the available project documentation and none are stated here.

VIII. Experimental Methodology

The assembled prototype was evaluated through a sequence of subsystem tests followed by combined operation on test plots. The objective of the evaluation was to establish whether each subsystem met the functional requirement placed on it by the architecture, and whether the integrated machine could execute the intended agricultural operations under field conditions. The measurements reported in this section are those recorded during project testing; they have not been independently reproduced.

A. Power System Test

The power subsystem was assessed by charging the battery from the photovoltaic panel under sunlight and subsequently operating the machine on stored energy until the actuators could no longer be sustained. Charging the 12 V, 1.2 Ah battery to full capacity from the 12 V, 5 W panel required 4 to 5 hours of sunlight. The stored charge then supported 6 to 8 hours of continuous operation of the base movement and tool functions. The ratio between these two intervals is the critical result of the test, since it determines whether a single day's insolation can support a full working session.

B. RF Communication Test

The command link was characterised by operating the transmitter at increasing separations from the robot in open field and observing whether issued commands were executed. Stable 433 MHz communication was achieved at distances of 50 to 100 m, with less than 1% signal loss recorded during testing. Testing was conducted in open-field conditions; performance in the presence of dense vegetation, structures or competing emitters in the band was not characterised.

C. Motor Performance Test

Actuator performance was assessed by commanding each function in turn and observing the resulting motion. The base motors, driven through the first L293D stage, produced a traversal speed of approximately 0.2 m/s. The cutter and shaft motors, driven through the second stage, operated at approximately 200 to 300 rpm. Directional control through the H-bridge stages was found to be precise, with forward, reverse and turning commands producing the expected motion. Minor overheating of the driver devices was observed under sustained load and was contained by their internal protection.

D. Agricultural Task Test

The three implemented agricultural functions were exercised individually. Navigation was assessed by manoeuvring the machine across the plot under remote command, confirming that the four-motor base could traverse the working surface and be positioned as required. Cutting was assessed by engaging the cutter element on standing material, and digging by engaging the shaft element with the soil surface; both were found effective at the operating speeds recorded above. Irrigation was not among the functions tested.

E. Overall Prototype and Field Test

Combined operation was evaluated on test plots by performing navigation, cutting and digging in sequence under continuous remote control. The multi-task operation reduced manual labour by 70% relative to performing the same operations by hand on those plots. The machine consumed no fuel during operation, drawing entirely on stored solar energy. The platform was observed to be robust against the vibration generated by the tool actuators, and no structural or connection failures were reported. The results of the complete evaluation are consolidated in Table 3.

IX. Results and Discussion

Table 1 lists the major hardware components of the implemented prototype and their functions. Table 2 summarises the system specifications, and Table 3 consolidates the experimental results reported during testing. Table 4 positions the implementation relative to the comparable systems reviewed in Section II.

Table 1. Major hardware components of the implemented prototype

Subsystem	Component	Function in the implemented system
Generation	Photovoltaic panel, 12 V / 5 W	Converts incident solar radiation into charging current for the battery
Storage	Rechargeable battery, 12 V / 1.2 Ah	Buffers generated energy; sole supply during operation
Regulation	78XX three-terminal positive regulator	Derives the 5 V logic rail; provides thermal and short-circuit protection
Control	ATmega328 / ATmega328P microcontroller	Decodes received commands and generates driver control signals
Timing	16 MHz crystal with loading capacitors	Provides the controller clock reference
Reset	Resistor–capacitor reset network	Ensures deterministic controller start-up
Communication	433 MHz RF transmitter and receiver pair	Carries the command word from the remote unit to the robot
Command entry	Four push buttons with parallel-to-serial encoder	Generates the command word at the operator end
Actuation drive	L293D quadruple half-H driver (×2)	Switches motor current and sets direction for traction and tools
Traction	Four DC geared motors	Provide forward, reverse and turning motion of the base
Tools	Cutter motor and shaft motor	Perform cutting and digging operations
Irrigation provision	Pump output via power MOSFET stage	Present in the circuit design; not experimentally validated
Integration	Single-sided printed circuit board	Carries the controller, regulation, receiver and driver interconnections

Table 2. System specifications of the implemented prototype

Parameter	Specification
Photovoltaic panel	12 V, 5 W
Battery	12 V, 1.2 Ah rechargeable
Logic supply rail	5 V, derived through 78XX-series regulator
Motor supply rail	12 V, taken directly from the battery
Controller	ATmega328 / ATmega328P, 16 MHz external crystal
Wireless link	433 MHz RF transmitter and receiver
Command interface	Four push buttons with parallel-to-serial encoder
Motor driver stages	Two L293D devices (traction; tools)
Base motors	Four DC geared motors
Tool actuators	Cutter motor and shaft (digging) motor
Implemented functions	Movement, cutting, digging
Autonomous navigation	Not implemented
Sensing subsystem	Not implemented

Table 3. Experimental results reported during project testing

Parameter	Reported result
Solar panel	12 V, 5 W
Battery	12 V, 1.2 Ah
Battery charging time	4–5 hours of sunlight
Continuous operation	6–8 hours
RF communication range	50–100 m in open field
RF signal loss	Less than 1%
Base motor speed	Approximately 0.2 m/s
Cutter / shaft motor speed	Approximately 200–300 rpm
Reduction in manual labour	70% on test plots
Fuel consumption	Zero during operation
Thermal behaviour	Minor overheating, contained by L293D protection
Structural robustness	No failures reported under actuator vibration

Table 4. Comparison of reviewed approaches with the proposed implementation

System	Control interface	Functions	Reported limitation
Kamble et al. [1]	Arduino-based control, solar supply	Soil tilling, seeding	Restricted remote-control range; reduced battery endurance under cloud
Patil et al. [2]	ATmega328 with Bluetooth link	Ploughing, weeding, spraying	Bluetooth interference in open field; difficulty on rugged terrain
Chadalavada [3]	Semi-automated, no remote operation	Digging, cutting	Lacks full automation and remote-operation capability
Proposed implementation	ATmega328P with dedicated 433 MHz RF link	Movement, cutting, digging	Remotely operated rather than autonomous; no sensing subsystem

A. Discussion

The relationship between the reported charging and operating intervals is the most consequential of the results. A charging period of 4 to 5 hours yielding 6 to 8 hours of continuous operation means that a single day of adequate insolation supports a working session longer than the charge that produced it, which in turn indicates that the machine can be operated on a daily cycle without any external energy input. This is the condition that makes deployment feasible in locations without a dependable grid connection. The result should not be over-generalised: it reflects the duty cycle exercised during testing, and sustained heavy tool loading would draw down the 1.2 Ah reserve more rapidly.

The wireless results demonstrate that the control architecture is sound for the intended mode of use. A working separation of 50 to 100 m with less than 1% signal loss exceeds the distance across which an operator can usefully observe a small machine directly, so the link is not the factor limiting the working envelope. This addresses precisely the weakness identified in the Bluetooth-based system of [2], and confirms that the choice of a dedicated sub-gigahertz channel was the appropriate response to the reported interference behaviour of consumer-protocol links in open ground.

Mobility and agricultural functionality are established at modest but adequate levels. A traversal speed of approximately 0.2 m/s is deliberately low, reflecting the torque bias of the geared drive and suiting a machine positioned by discrete operator commands rather than driven continuously. Tool speeds of 200 to 300 rpm proved sufficient for the cutting and digging performed on the test plots. That both traction and tool functions could be commanded during the same session, without either constraining the other, validates the decision to assign them to separate H-bridge stages.

The 70% reduction in manual labour recorded on the test plots is the clearest indication of practical value, though its interpretation requires care. The figure reflects a specific set of operations on a specific set of plots and is not a general productivity coefficient; it does, however, indicate that the machine displaces a substantial proportion of the physical effort those operations would otherwise require. The environmental benefit is more directly attributable: operation consumed no fuel at all, so the emissions and recurring fuel cost associated with an equivalent engine-driven implement are eliminated outright rather than merely reduced.

Taken together, the results demonstrate the feasibility of solar-assisted, RF-controlled multipurpose field machinery at this scale and show promising performance across the functions implemented. They indicate practical potential for small-holding applications rather than establishing commercial readiness: the evaluation covered a limited number of test plots over short durations, the thermal behaviour of the driver stages under prolonged heavy load requires further characterisation, and durability across a full cropping season has not been assessed.

X. Advantages and Applications

The principal advantage of the implemented system is energy autonomy. Photovoltaic generation with battery storage eliminates fuel consumption entirely and removes any dependence on the electricity grid during operation, which reduces recurring operating cost to effectively zero and permits use in areas where grid supply is limited or unavailable. The absence of an internal-combustion engine also removes the associated emissions, noise and routine maintenance burden.

Wireless operation confers a second set of advantages. Because the operator directs the machine from a distance, exposure to the cutting and digging implements and to the dust and heat of the working environment is reduced. The multipurpose architecture allows movement, cutting and digging to be performed by a single platform rather than by three separate implements, with traction and tool stages exercisable concurrently. The build is compact, portable and assembled from low-cost, widely available components, keeping both acquisition and repair cost within reach of small-scale users.

The corresponding applications are those of small and medium landholdings. The platform suits crop cutting and weed trimming within narrow rows, soil digging and loosening on compact plots, and controlled movement across the field for positioning and general agricultural maintenance. It is well matched to off-grid farmland where recharging depends on the panel alone, and to plots whose size does not justify the deployment of tractor-mounted machinery. Applications that would require environmental sensing, localisation or unattended autonomous operation are outside the scope of the present prototype and are identified in Section XII as future work.

XI. Limitations

The prototype is remotely operated and not autonomous. Every action originates in an operator command, so the machine cannot execute a task unattended, follow a row, or plan coverage of a plot. The working envelope is consequently bounded by the operator's line of sight as well as by the radio range, and one operator remains occupied for the full duration of any operation.

Energy availability is a second constraint. Charging depends entirely on sunlight, so overcast weather, seasonal variation in insolation and shading of the panel all extend the charging interval. With a 1.2 Ah reserve and no alternative charging path, a sequence of low-sunlight days will curtail the available operating time, and sustained high-load tool work will deplete the battery faster than the duty cycle exercised during testing.

The communication link, although adequate over the tested range, was characterised only in open field. The 433 MHz band is shared with other equipment, and range and reliability may degrade in the presence of competing emitters, dense vegetation, structures or unfavourable terrain; no characterisation under those conditions is available. Since the link carries no return channel, the operator receives no status telemetry from the machine.

Mechanical performance is terrain-dependent. Traction, ground clearance and the effectiveness of the digging element vary with soil condition, slope and surface obstructions, none of which were varied systematically during testing. Minor overheating of the driver stages was observed under sustained load; although contained by internal protection, this indicates that thermal margin at the driver stage is limited. The prototype also incorporates no sensing of any kind — no soil, obstacle, position or battery-state measurement is available to either the controller or the operator.

Finally, the experimental evidence itself is limited in extent. Testing covered a small number of plots over short durations, and no data are available on performance across different crops, soil types or seasons, nor on long-term reliability. Broader field validation would be required before conclusions could be drawn about operational durability. These constraints describe the system as built and should be distinguished from the enhancements proposed in the following section, which were not implemented.

XII. Future Scope

The following enhancements are identified in the project documentation as directions for further development. It should be stated clearly that none of them forms part of the prototype reported in this paper, and no experimental results relating to them are presented.

Autonomous navigation is the most substantial proposed extension, replacing continuous operator direction with self-guided traversal of the plot. IoT-based soil monitoring would add sensing of soil parameters and communicate the resulting measurements beyond the machine, and real-time monitoring would provide the operator with status and performance information that the present unidirectional link cannot carry. AI-assisted decision-making is proposed as a means of selecting operations according to observed field conditions rather than by explicit command. Alongside these, further software optimisation of the control firmware and adaptation of the tool mechanisms to different crop conditions are identified as incremental improvements to the existing platform.

Each of these directions would require hardware not present in the current build — sensing, localisation, additional computation or a bidirectional communication channel — and would need to be evaluated against the energy budget established in Section IX, since any added subsystem draws on the same 1.2 Ah reserve that presently supports the actuators.

XIII. Conclusion

This paper has presented the design, implementation and experimental evaluation of a solar-powered multipurpose agricultural robot for small and medium-scale field operations. The prototype integrates a 12 V, 5 W photovoltaic panel with a 12 V, 1.2 Ah battery and a regulated distribution stage to provide complete energy autonomy during operation; an ATmega328P microcontroller with external oscillator and reset circuitry as the central controller; a 433 MHz radio link with a four-button encoder-based remote for wireless command entry; and two L293D H-bridge driver stages that separate traction from tool actuation, operating four base motors together with cutter and shaft actuators. Movement, cutting and digging were implemented and integrated onto a single printed circuit board assembly suitable for field use.

Experimental testing of the assembled prototype established a battery charging time of 4 to 5 hours of sunlight yielding 6 to 8 hours of continuous operation, a stable wireless link over 50 to 100 m in open field with less than 1% signal loss, a base traversal speed of approximately 0.2 m/s, tool speeds of 200 to 300 rpm, and a 70% reduction in manual labour on the test plots, all achieved with zero fuel consumption.

These results demonstrate the feasibility of combining photovoltaic generation with low-cost embedded control and radio-frequency command transfer in a compact agricultural platform, and indicate practical potential for reducing both the labour intensity and the environmental burden of small-holding cultivation. The prototype remains operator-directed rather than autonomous and carries no sensing subsystem, and the evaluation reported here covers a limited range of field conditions; broader validation and the sensing, navigation and monitoring extensions outlined in Section XII represent the necessary next stages of development.

References

[1] Kamble et al., “Development of a Solar-Powered Autonomous Agricultural Robot,” 2024. (Bibliographic details as cited in the source project documentation.)

[2] H. Patil et al., “Solar Powered Autonomous Multipurpose Agriculture Robot,” International Journal of Innovative Research in Science, Engineering and Technology (IJIRSET), 2024. [Online]. Available: https://www.ijirset.com/upload/2024/may/418_Solar.pdf

[3] H. Chadalavada, “Solar powered semi-automated multipurpose agriculture tool,” 2021. (Bibliographic details as cited in the source project documentation.)

[4] V. R. Beldar et al., “Solar-Powered, Multi-Use, Remote-Controlled Farm Robot,” IEEE, 2024. [Online]. Available: https://ieeexplore.ieee.org/document/10716121/

[5] “Design and Development of Solar Powered Automated Agriculture Bot,” International Journal for Research in Applied Science and Engineering Technology (IJRASET), 2024. [Online]. Available: https://www.ijraset.com/research-paper/development-of-solar-powered-automated-agriculture-bot

[6] “Solar Powered Automated Multi-Tasking Agricultural Robot,” IJIREEICE, 2024. [Online]. Available: https://ijireeice.com/papers/solar-powered-automated-multi-tasking-agricultural-robot/

[7] “Smart Solar Powered Web Controlled Multi-function Agribot,” International Journal of Engineering Research and Technology (IJERT). [Online]. Available: https://www.ijert.org/smart-solar-powered-web-controlled-multi-function-agribot

[8] “Solar-Powered Multipurpose Agricultural Robot,” project repository. [Online]. Available: https://github.com/devanshu3/Solar_Powered_Multipurpose_Agricultural_Robot